AGU PUBLICATIONS

JGR

Journal of Geophysical Research: Atmospheres

RESEARCH ARTICLE
10.1002/2017JD027833

Key Points:
- The absorption enhancement of BC aggregates due to coating of organics is numerically investigated based on recent observations
- The effects of detailed coating microphysics on the absorption enhancements of partially coated BC particles are systematically studied
- This study provides a plausible reconciliation of largely variable absorption enhancements with highlighting BC coating volume fraction

Correspondence to:
X. Zhang and M. Mao,
xlnzhang@nuist.edu.cn;
mmao@nuist.edu.cn

Citation:
Zhang, X., Mao, M., Yin, Y., & Wang, B. (2018). Numerical investigation on absorption enhancement of black carbon aerosols partially coated with nonabsorbing organics. *Journal of Geophysical Research: Atmospheres*, *123*, 1297–1308. https://doi.org/10.1002/2017JD027833

Received 25 JUL 2017
Accepted 3 JAN 2018
Accepted article online 6 JAN 2018
Published online 26 JAN 2018

Numerical Investigation on Absorption Enhancement of Black Carbon Aerosols Partially Coated With Nonabsorbing Organics

Xiaolin Zhang[1,2,3], Mao Mao[1,2,3], Yan Yin[1,2], and Bin Wang[1,3]

[1]Earth System Modeling Center/Collaborative Innovation Center on Forecast and Evaluation of Meteorological Disasters/Key Laboratory for Aerosol-Cloud-Precipitation of China Meteorological Administration/Joint International Research Laboratory of Climate and Environment Change/Key Laboratory of Meteorological Disaster, Ministry of Education, Nanjing University of Information Science & Technology, Nanjing, China, [2]School of Atmospheric Physics, Nanjing University of Information Science & Technology, Nanjing, China, [3]International Pacific Research Center, University of Hawaii at Mānoa, Honolulu, HI, USA

Abstract This study numerically evaluates the effects of aerosol microphysics, including coated volume fraction of black carbon (BC), shell/core ratio, and size distribution, on the absorption enhancement (E_{ab}) of polydisperse BC aggregates partially coated by organics, which is calculated by the exact multiple-sphere T-matrix method. The coated volume fraction of BC plays a substantial role in determining the absorption enhancement of partially coated BC aggregates, which typically have an E_{ab} in the range of ~1.0–2.0 with a larger value for larger coated volume fraction of BC as the shell/core ratio, BC geometry, and size distribution are fixed. The shell/core ratio, BC geometry, and size distribution have little impact on the E_{ab} of coated BC with small coated volume fraction of BC, while they become significant for large coated volume fraction of BC. The E_{ab} of partially coated BC particles can be slightly less than 1.0 for the large BC in the accumulation mode exhibiting large shell/core ratio and small coated volume fraction of BC, indicating that the absorption shows even slight decrease relative to uncoated BC particles. For partially coated BC aggregates in the accumulation and coarse modes, the refractive index uncertainties of BC result in the E_{ab} differences of less than 9% and 2%, respectively, while those of organics can induce larger variations with the maximum differences up to 22% and 18%, respectively. Our study indicates that accounting for particle coating microphysics, particularly the coated volume fraction of BC, can potentially help to understand the differences in observations of largely variable absorption enhancements over various regions.

1. Introduction

Black carbon (BC) aerosols, largely produced due to fossil fuel demands, are ubiquitous in the atmosphere and have profound effects on the environment and climate (Mao et al., 2014; Myhre, 2009; Ramanathan & Carmichael, 2008; Zhang et al., 2015). As a key short-lived climate forcer, BC contributes significant positive radiative forcing, which is identified as the second most important contributor to global warming after CO_2 (Intergovernmental Panel on Climate Change, 2013). Once emitted into ambient air, BC particles can be coated with secondary aerosol species (e.g., organics and sulfate) through the aging process, and their absorption cross section can be enhanced (Shiraiwa et al., 2010). Currently, the results of absorption enhancement (E_{ab}) of aged BC particles from available experimental, theoretical, modeling, and field studies are inconsistent, leading to large uncertainties in assessing aerosol radiative forcing (Bond et al., 2013).

The absorption enhancement of BC due to coatings has been confirmed by laboratory studies conducted under controlled conditions, which yield a broad range of E_{ab}, varying from 1.05 to 3.5 (Khalizov et al., 2009; Xue et al., 2009; Shiraiwa et al., 2010; Bueno et al., 2011; Qiu et al., 2012; Bond et al., 2013; Khalizov et al., 2013). The resulting large variation among detailed laboratory experiments indicates that the absorption enhancement of coated BC strongly depends on coating microphysics, such as coating materials, particle morphology, composition ratio, and size distribution. While the laboratory experiments may not represent adequately ambient BC conditions in the atmosphere, field measurements have been implemented to reveal the absorption enhancement of coated BC. Naoe et al. (2009) report an absorption

enhancement of 1.1–1.4 because of coatings on BC at a suburban site in Japan. Similar results are observed in downtown Toronto, Canada, which present that the coating enhances BC absorption by up to 45% (Knox et al., 2009). The E_{ab} ranging from ~1.4 in fresh combustion emissions to ~3 for aged BC particles, with a mean value of 2.25, are found in a regional rural site over the North China Plain (NCP) (Cui et al., 2016). A distinct diurnal pattern of E_{ab} is even reported recently, with E_{ab} of 1.3 ± 0.3 in the morning, rising to 2.2 ± 1.0 in the afternoon, and dropping to 1.5 ± 0.8 during the evening-night, at an urban area, Jinan, in the NCP (Chen et al., 2017). Meanwhile, Cappa et al. (2012) present a negligible absorption enhancement of only 6% for ambient BC aerosols under a variable mixing state based on field measurements over California, USA.

The large variability of E_{ab} from field observations, implying its complexity in ambient air, may be determined by the complicated microphysics of coated BC, since E_{ab} is source-dependent and regionally dependent (S. Liu et al., 2015). Based on measurements of BC spherical equivalent core diameter (D_c) and coating thickness with a single-particle soot photometer (SP2), the shell/core ratio D_p/D_c (spherical equivalent particle diameter divided by BC core diameter) is observed to be 1.1–2.1 in London (D. Liu et al., 2015), whereas it is in the range of 2.1–2.7 in Beijing (Zhang et al., 2016). For the morphology of BC particles released from biomass burning, China et al. (2013) quantify that ~50% are heavily coated (embedded), ~34% are partially coated, ~12% have inclusions, and ~4% are bare. The mixing state measurement over northwestern China depicts that 48.6% of measured BC particles are coated with nonrefractory materials in polluted atmosphere (Wang et al., 2014). The observation of aged BC aerosols shows partially coated morphologies dominated at a remote marine free troposphere site in Portugal (China et al., 2015). These various coating morphologies and mixing state of aged BC particles may substantially affect their absorption enhancements, accounting for the large E_{ab} variation over different regions.

Numerical simulation is able to shed some light on the mechanism responsible for the complex absorption enhancements of coated BC aerosols with large variability measured in ambient air. Core-shell Mie theory is employed by many studies, assuming coated BC particles with a concentric spherical configuration and indicating that absorption enhancements up to 3 are plausible (e.g., Bond et al., 2006; Schwarz et al., 2008). This simple concentric spherical core-shell model may be only suitable for those severely polluted environments, such as the NCP, where BC ages with a short timescale and large sulfate formation rate is induced by the aqueous oxidation of SO_2 by NO_2 (Peng et al., 2016; Wang et al., 2016). He et al. (2015) find that the absorption enhancement of BC coated by sulfuric acid varies during aging with a numerical investigation at three monodisperse sizes (i.e., mobility diameters of 155, 245, and 320 nm). Adachi and Buseck (2013) report that modeled BC particles externally attached to nonabsorbing materials have E_{ab} ~1, i.e., absorption showing no increase relative to uncoated BC aggregates. The observed irregular BC coating morphologies in ambient atmosphere can generally be classified into three types: fully coated, partially coated, and externally attached (e.g., Adachi & Buseck, 2013, China et al., 2013, 2015). Although significant theoretical calculations have been carried out to study the variation of BC absorption due to externally attached to, or fully coated by nonabsorbing materials, few research focuses on the numerical investigation of the absorption enhancement of partially coated BC aerosols, which significantly limits our ability to understand the model-observation discrepancies and to perform accurate radiative transfer calculations.

Here numerical investigations of the absorption enhancement of polydisperse BC aggregates partially coated by organics are systematically presented. An exact multiple-sphere T-matrix method (MSTM) is employed to numerically calculate the absorption properties of partially coated BC aggregates and then their absorption enhancements. The objective is to evaluate the effects of coating microphysics, including coated volume fraction of BC, shell/core ratio, and size distribution, on the absorption enhancements of partially coated BC particles, which hopefully benefits our understanding of the mechanism responsible for the model-observation discrepancies and refining estimates of aerosol radiative forcing. The sensitivities of the absorption enhancements due to the refractive index uncertainties of BC and organics are also stressed. This study is novel in that (1) the absorption enhancements of partially coated BC particles affected by their coating microphysics are systematically investigated based on recent observations and (2) it provides a plausible reconciliation of the conflicting results of largely variable absorption enhancements observed over various regions with highlighting BC coating volume fraction.

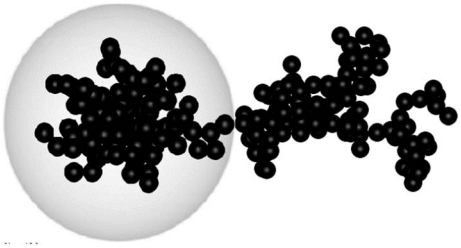

Figure 1. Sketch map of partially coated black carbon geometry. An example of fractal black carbon aggregates, containing 200 monomers, is partially coated by nonabsorbing organics with coated volume fraction of black carbon being 0.5.

2. Methodology: Models and Numerical Simulation

Freshly emitted BC particles are often observed to be loose cluster-like aggregates with numerous similar-sized spherical monomers (e.g., Li et al., 2016), and the fractal aggregates have been successfully employed to construct these BC geometries, following the well-known statistical scaling law (e.g., Sorensen, 2001):

$$N = \mathrm{k}_0 \left(\frac{R_g}{a}\right)^{D_f}, \tag{1}$$

$$R_g = \sqrt{\frac{1}{N}\sum_{i=1}^{N} R_i^2}, \tag{2}$$

where the monomer number of an aggregate (N), monomer radius (a), fractal prefactor (k_0), and fractal dimension (D_f) control the morphology of a BC aggregate. R_g is the gyration radius, which measures the overall spatial size of an aggregate, and r_i denotes the distance from the ith monomer to the mass center of the aggregate.

During the aging process, BC aggregates can be coated with organics (e.g., Schwarz et al., 2008; Tritscher et al., 2011), and their chain-like aggregates tend to collapse into more compact clusters (Coz & Leck, 2011; Zhang et al., 2008). The fractal dimensions of fresh BC aggregates are generally less than 2, whereas they are almost 3 for aged BC aerosols (Liu et al., 2008). This study mainly considers the BC aggregates partially coated with organics, and the coated volume fraction of BC (F) is an important parameter describing the coating state of BC and organics, which is given following the equation below:

$$F = \frac{V_{\mathrm{BC\ inside}}}{V_{\mathrm{BC}}}, \tag{3}$$

where $V_{\mathrm{BC\ inside}}$ is the volume of BC monomers inside organics, while V_{BC} is the volume of the overall BC aggregate, including BC monomers both inside and outside the coating. The partially coated BC aggregates typically have a coated volume fraction of BC of $0 < F < 1$, while the externally attached and fully coated BC particles show $F = 0$ and $F = 1$, respectively. The organics are treated as spheres that are coated to the BC fractal aggregates with different coated volume fractions of BC, and some observations of individual aged BC particles actually do show this spherical coating geometry (e.g., Alexander et al., 2008, Wu et al., 2016, Zhang et al., 2008).

To construct this inhomogeneous internal-mixed particle, we first generate a BC fractal aggregate and then add a spherical coating of organics. The BC aggregates are generated based on a tunable particle-cluster aggregation algorithm from Skorupski et al. (2014). The k_f value of BC is assumed to be 1.2 (Sorensen, 2001), while two D_f values of 1.8 and 2.8 are chosen to represent lacy and compact aged BC aggregates (Cheng et al., 2014; Wu et al., 2016). The radius a of BC aggregate monomers can change over a range of about 10–25 nm (Bond & Bergstrom, 2006), whereas the monomer number N is observed to vary up to approximately 800 (Adachi & Buseck, 2008). As the monomer size has a rather weak effect on BC scattering and absorption after D_f being fixed (He et al., 2015; Liu & Mishchenko, 2007), we choose two N values of 200 and 800 as examples for accumulation and coarse particles, respectively. After a BC aggregate being generated, the coating sphere of organics is placed to coat the BC aggregate from one side to the other until an expected F is reached. To avoid overlapping, some BC aggregate monomers are slightly moved, but their aggregate geometry is still kept. It should be noticed that the BC monomer movements to avoid overlapped spheres after being coated have led to a slight alteration of the fractal dimension of the BC aggregate. The sketch map of the BC aggregates partially coated by nonabsorbing organics is depicted in Figure 1.

Many numerical methods, such as the multiple-sphere T-matrix method (Mackowski, 2014), discrete dipole approximation (Draine & Flatau, 1994), finite difference time domain method (Yang & Liou, 1996), and geometric-optics surface-wave (GOS) approach (Liou et al., 2014; Liou & Yang, 2016), can be applied to compute the optical properties of coated BC aggregates. Among these optical methods, the exact MSTM seems to be fastest, which is in the framework of the T-matrix method, and is employed to accurately calculate the random-orientation optical properties of partially coated BC aggregates in this study. The MSTM can be

Table 1
Key Microphysical Properties of BC Aggregates Partially Coated by Organics

Parameters		Applied values
F		0.01, 0.25, 0.5, 0.75, 0.99
D_p/D_c		1.1, 1.5, 1.9, 2.3, 2.7
BC D_f		1.8, 2.8
Size distribution	r_g, μm	0.075, 0.75
	σ_g	1.59, 2.0
Refractive index	BC	1.85–0.71*i*
	Organics	1.55-0*i*

applied to arbitrary configurations of spheres situated internally or externally to other spheres, with the only limitation that the spherical surfaces are nonoverlapping (Mackowski & Mishchenko, 1996). The robust MSTM has already been widely employed for numerous numerical investigations of optical properties of fractal aggregates (e.g. Dlugach & Mishchenko, 2015; He et al., 2016; Mishchenko et al., 2016; Zhang et al., 2017).

For ambient atmospheric applications, bulk aerosol optical properties averaged over a certain particle size distribution are meaningful. This study considers an ensemble of BC aggregates with different sizes but the same coating fraction of organics (i.e., same D_p/D_c), and a lognormal size distribution is assumed following the form of

$$\mathrm{n}(r) = \frac{1}{\sqrt{2\pi} r \ln(\sigma_g)} \exp\left[-\left(\frac{\ln(r) - \ln(r_g)}{\sqrt{2}\ln(\sigma_g)}\right)^2\right], \tag{4}$$

where σ_g is the geometric standard deviation and r_g is the geometric mean radius (e.g., Yurkin & Hoekstra, 2007; Schwarz et al., 2008). Since particles in accumulation and coarse modes contribute dominated light absorption, we only consider coated BC aerosols in both modes. For the accumulation mode, the radius range is set as 0.05–0.5 μm, while the coarse radius range is assumed to be 0.5–2.5 μm as ambient aerosols with size larger than 5 μm are few (X. Zhang et al., 2012; Zhang, Huang, Rao, et al., 2013; Zhang, Huang, Zhu, et al., 2013; Zhang et al., 2014; Zhang & Mao, 2015).To better understand the absorption enhancement of partially coated BC at different particle size mode, size distributions in accumulation and coarse modes are applied separately, which are similar to those used in the aerosol-climate models (K. Zhang et al., 2012). In this study, we consider the size distributions of coated BC aggregates (i.e., BC-organics internal mixtures) with r_g of 0.075 μm and 0.75 μm and σ_g of 1.59 and 2.0 in accumulation and coarse modes, respectively (K. Zhang et al., 2012). As a particle size distribution is given, the bulk absorption cross section of coated BC can be easily calculated with the following equation:

$$\langle C_{\mathrm{abs}} \rangle = \int_{r_{\min}}^{r_{\max}} C_{\mathrm{abs}}(r) n(r) d(r) \tag{5}$$

Given that the ensemble-averaged absorption cross section is obtained, the absorption enhancement E_{ab} is given in the form of:

$$E_{ab} = \frac{C_{\mathrm{particle}}}{C_{\mathrm{bare\ BC}}}, \tag{6}$$

where C_{particle} is the bulk absorption cross section of BC aggregates coated by organics, while $C_{\mathrm{bare\ BC}}$ is the bulk absorption cross section of the same bare BC aggregates (without coating of organics).

The absorption enhancement of partially coated BC aggregates is investigated at an incident wavelength of 550 nm, and related refractive indices of BC and organics are assumed as 1.85–0.7l*i* (Bond & Bergstrom, 2006) and 1.55-0*i* (Chakrabarty et al., 2010), respectively. The shell/core ratio D_p/D_c of coated BC is assumed to be in the range of 1.1–2.7 on the basis of the SP2 measurements in London (D. Liu et al., 2015) and Beijing (Zhang et al., 2016). A summary of the key parameters of coated BC applied in this study is listed in Table 1. With the inhomogeneous coated BC model defined, which depicts quite realistic geometries, it is possible to study the absorption enhancement of partially coated BC aerosols with more details. It should be noticed that with significant uncertainties in the morphology of coating of organics, our results and conclusions are specified for BC with the above mentioned spherical coating. However, for coated BC particles, the simple spherical coating is found to have similar effects on optical properties to those based on more complicated coating structures (e.g., Dong, Zhao, & Liu, 2015; F. Liu et al., 2015). Therefore, it is expected that the uncertainty in the absorption enhancement of coated BC due to the morphology of coating of organics would be limited. We only focus on the effects of coated volume fraction of BC, particle shell/core ratio, and size distribution on the absorption enhancement of partially coated BC, and thus, the assumptions regarding the morphology of spherical coating of organics would not qualitatively change or overshadow our conclusions.

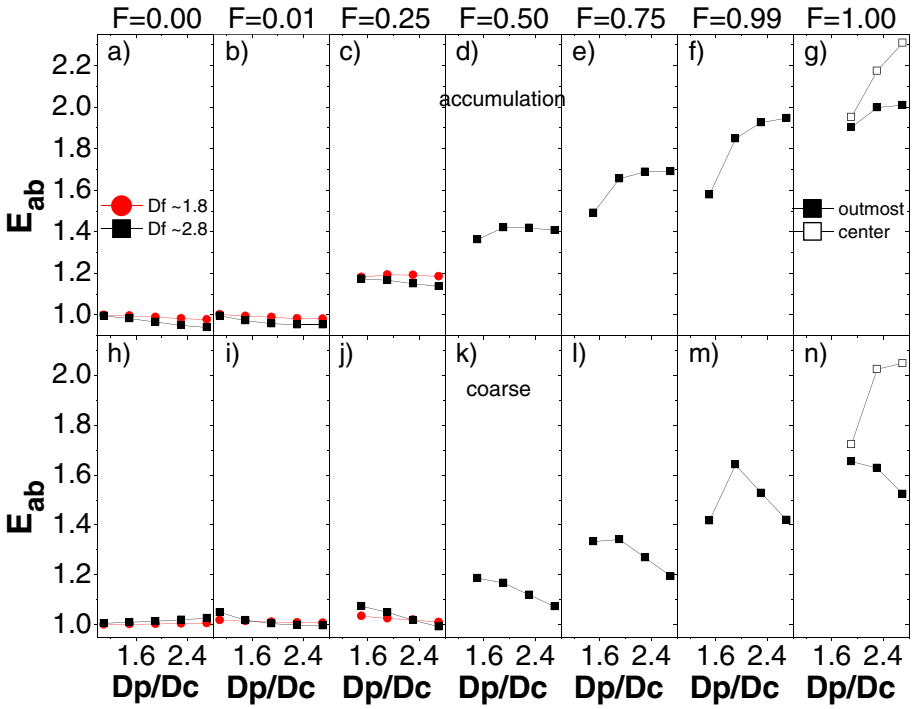

Figure 2. Absorption enhancement (E_{ab}) of BC aggregates coated with organics as a function of shell/core ratio (D_p/D_c, spherical volume-equivalent particle diameter/BC core diameter), in (a–g) accumulation and (h–n) coarse modes, respectively. The coated volume fractions of BC (F) of 0.0, 0.01, 0.25, 0.5, 0.75, 0.99, and 1.0 are considered (from left to right). The black squares and red circles indicate BC fractal dimensions of ~2.8 and ~1.8, respectively. For coating cases with $F = 1$, the black solid squares denote BC aggregates locating at an outmost position close to coating boundary, while the black open squares indicate BC at the particle geometric center.

3. Results and Discussion

3.1. Effect of BC Coating Structure on E_{ab}

Figure 2 depicts the absorption enhancements of BC aggregates partially coated by organics with different coated volume fractions of BC at different shell/core ratios. Five coated volume fractions of BC (i.e., $F = 0.01$, 0.25, 0.5, 0.75, and 0.99) and two BC fractal dimensions (i.e., $D_f \approx 1.8$ and 2.8) are considered. To show the whole effect of coated volume fraction of BC on E_{ab}, two fully coated structures (i.e., a concentric core-shell and an outmost off-center core-shell) and an externally attached structure are also illustrated in Figure 2 for comparison. The concentric core-shell structure denotes that the mass center of BC aggregates is located at the overall particle geometric center, while the outmost off-center core-shell structure indicates that BC aggregates are situated at an outmost position inside organics, which is close to coating boundary. The properties are averaged over an ensemble of BC-organics internal-mixed particles with the aforementioned size distributions for accumulation and coarse modes separately.

As shown in Figure 2, partially coated BC aggregates with more coated volume fractions of BC have larger E_{ab} for the same shell/core ratio, and the E_{ab} becomes more sensitive to the shell/core ratio with the increase of coated volume fraction of BC. Starting from BC fractal dimension of ~2.8, for a small coated volume fraction of BC with $F = 0.01$, values of E_{ab} are slightly less than 1.0 (in the range of 0.95–1.0) in accumulation mode, whereas they have close values between 1.0 and 1.05 in coarse mode. For a moderate coated volume fraction of BC with $F = 0.5$, values of E_{ab} are in the ranges of 1.3–1.4 and 1.1–1.2 in accumulation and coarse modes, respectively. With the coated volume fraction of BC reaching $F = 0.99$, the E_{ab} varies from 1.6 to 1.9 in accumulation mode, while it ranges from 1.5 to 1.7 in coarse mode. For externally attached BC-organic particles (see Figures 2a and 2h), their E_{ab} values are ~1.0, which are generally similar to those of BC aggregates with small coated volume fractions of BC. This is in line with the conclusion presented in Adachi and Buseck (2013) that BC particles attached to other materials hardly enhance their light absorption.

Surprisingly, in accumulation mode, the externally attached or partially coated BC aggregates with small coated volume fraction of BC have E_{ab} slightly less than 1.0, i.e., absorption showing even slight decrease relative to uncoated BC particles. One possible explanation for this result could be that these structures have a shadowing effect caused by nonabsorbing coating material that prevents photons from being absorbed by BC (He et al., 2015, 2016; Liu & Mishchenko, 2007). Compared with the partially coated structures, the fully coated BC structures give larger E_{ab} for fixed D_p/D_c in both accumulation and coarse modes. Among all fully coated BC aggregates (see Figures 2g and 2n), the E_{ab} given by the outmost off-center core-shell structure is lower than that given by the concentric core-shell structure with the same D_p/D_c. The E_{ab} of BC aggregates fully coated by organics with the concentric structure increases in the ranges of 2.0–2.3, 1.8–2.1 in accumulation and coarse modes, respectively, as D_p/D_c increases from 1.9 to 2.7. Nevertheless, the E_{ab} of the outmost off-center coated BC aggregates have close values in the ranges of 1.9–2.0 and 1.7–1.8 in accumulation and coarse modes, respectively. One can see that only those fully coated BC aggregates with a concentric structure and high shell/core ratios may have their E_{ab} larger than 2.0. The variation of E_{ab} on coated volume fraction of BC in accumulation mode is relatively stronger than that in coarse mode. The impact of D_p/D_c on the E_{ab} of coated BC is complicated, especially in coarse mode. In accumulation mode, with D_p/D_c increasing, the E_{ab} generally show monotonic decrease for $F > 0.5$, as opposed to the increase of E_{ab} for $F > 0.5$. The E_{ab} of coated BC is also sensitive to its BC fractal dimension, and the differences induced by different BC fractal dimensions are within 5% for externally attached or partially coated BC with small coated volume fraction of BC.

Generally, the absorption enhancement of BC aggregates due to coating of organics is sensitive to coated volume fraction of BC, particle geometry, and shell/core ratio, wherein the coated volume fraction of BC plays a more substantial role in determining the absorption enhancement. The E_{ab} of partially coated BC is less sensitive to particle geometry and shell/core ratio for less coated volume fraction of BC, and with coated volume fraction of BC being large, the results based on different D_p/D_c show significant differences. Specifically, for a fixed D_p/D_c, the externally attached or partially coated BC with small F have the lowest E_{ab} of ~1.0, followed by the partially coated BC with median F, and the fully coated BC have the largest E_{ab} with a value as high as ~2.0.

3.2. Effect of BC Refractive Index on E_{ab}

As elucidated in Bond et al. (2006), BC refractive indices (RIs) have significant uncertainties with an upper bound BC RI of 1.95–0.79*i* and a lower bound of 1.75–0.63*i*. The effect of BC RI uncertainties on the E_{ab} of BC aggregates (BC fractal dimension of ~2.8) partially coated by organics with the aforementioned size distributions is illustrated in Figure 3. The results based on BC RIs at the upper and lower bounds and the RI of aforementioned0 1.85-07l*i* are compared for three coated volume fractions of BC (i.e., F = 0.01, 0.05, and 0.99). For accumulation partially coated BC, the E_{ab} based on larger BC RI has larger value, and the E_{ab} differences due to BC RI uncertainties increase from almost 0% to 4–9% depending on D_p/D_c as F increases from 0.01 to 0.99. For coarse BC aggregates partially coated by organics, their E_{ab} values on the basis of three different BC RIs are in general agreement with differences within 2%. The absorptions of aged BC aerosols have strong dependences on BC refractive index (Liu et al., 2008; Scarnato et al., 2015), and variations of 20–40% and 10–17% are found based on the use of BC RIs at the upper and lower bounds for uncoated and coated BC aggregates, respectively (He et al., 2015). Nevertheless, the uncertainties of BC refractive index have little effect on the absorption enhancement of partially coated BC aggregates with differences within 9% and 2% in accumulation and coarse modes, respectively.

3.3. Effect of Refractive Index of Organics on E_{ab}

The laboratory observations have indicated that the refractive indices of secondary organic aerosols can vary between 1.35 and 1.61 due to their chemical and physical complexities, such as parent hydrocarbon, oxidation chemistry, and organics generation temperature (Chakrabarty et al., 2010; Kim & Paulson, 2013). To study the effect of refractive index of organics on the absorption enhancement of partially coated BC, three RIs of organics are considered, i.e., 1.35-0*i*, 1.44-0*i*, and the aforementioned 1.55-0*i*. Figure 4 illustrates the E_{ab} variations of partially coated BC aggregates (BC fractal dimension of ~2.8) due to different refractive indices of organics with the aforementioned size distributions for three coated volume fractions of BC (i.e., F = 0.01, 0.5, and 0.99). The E_{ab} of partially coated BC aggregates is enlarged, when the large refractive index of organics is

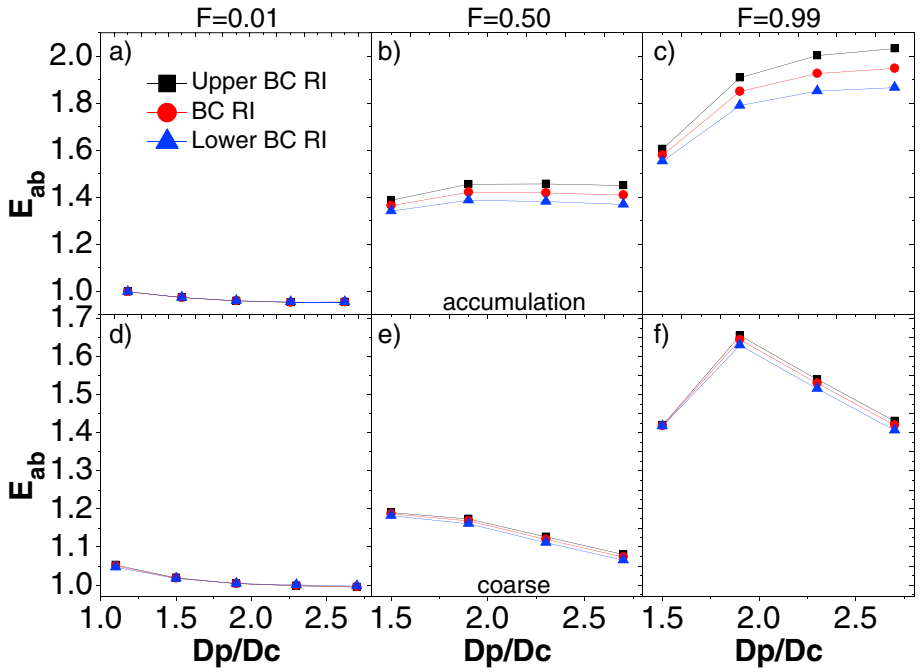

Figure 3. Absorption enhancement (E_{ab}) of BC aggregates partially coated by organics (BC fractal dimension of ~2.8) as a function of shell/core ratio (D_p/D_c), for (a–c) accumulation and (d–f) coarse modes, respectively. Three coated volume fractions of BC of 0.01, 0.5, and 0.99 are shown from left to right. Three BC refractive index (RIs) are considered, including a popular RI of 1.85–0.7*i* (red circles), an upper bound RI of 1.95–0.79*i* (black squares) and a lower bound RI of 1.75–0.63*i* (blue triangles).

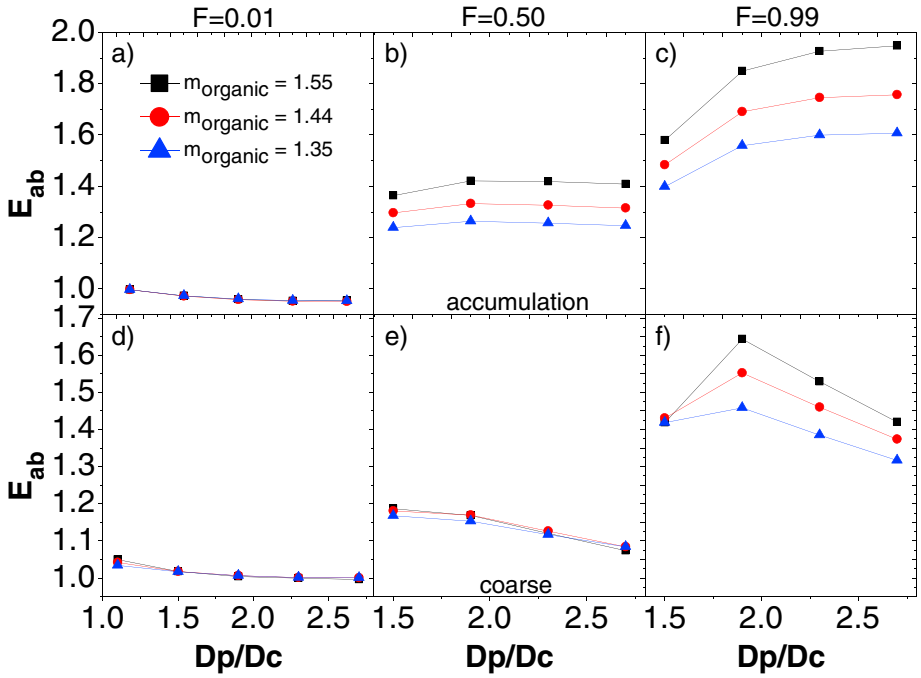

Figure 4. Absorption enhancement (E_{ab}) of BC aggregates partially coated by organics (BC fractal dimension of ~2.8) as a function of shell/core ratio (D_p/D_c), for (a–c) accumulation and (d–f) coarse modes, respectively. Three coated volume fractions of BC of 0.01, 0.5, and 0.99 are depicted from left to right. Three refractive indices (RIs) of organics are considered, i.e., 1.55-0*i* (black squares), 1.44-0*i* (red circles), and 1.35-0*i* (blue triangles).

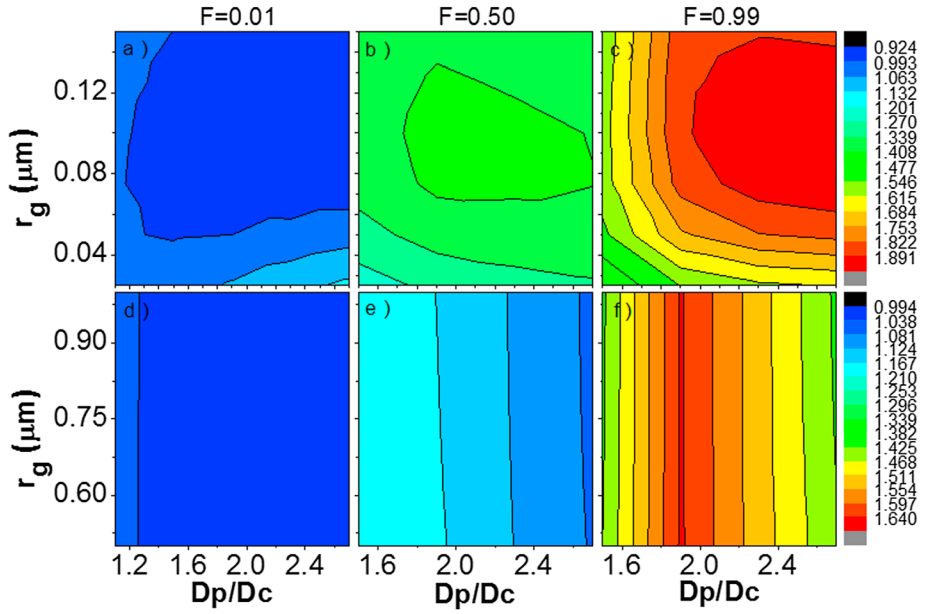

Figure 5. Absorption enhancement (E_{ab}) of partially coated BC aggregates (BC fractal dimension of ~2.8) with different shell/core ratio (D_p/D_c) and particle size distribution for (a–c) accumulation and (d–f) coarse modes, respectively. Three coated volume fractions of BC of 0.01, 0.5, and 0.99 are shown from left to right. The geometric standard deviations (σ_g) for applied lognormal distribution are 1.59 and 2.0 for accumulation and coarse aerosols, respectively.

considered. As F augments from 0.01 to 0.99, the E_{ab} of partially coated BC and its differences due to varying refractive indices of organics increase dramatically. In accumulation mode, the E_{ab} differences caused by different RIs of organics are less than 1% for F = 0.01, followed by differences of 10–13% for F = 0.5, while the differences reach 13–22% for F = 0.99, depending on D_p/D_c. Meanwhile, larger D_p/D_c generally leads to larger E_{ab} differences in accumulation mode when different RIs of organics are utilized. The E_{ab} differences induced by different RIs of organics in coarse mode show similar patterns to those in accumulation mode, and the differences can be up to 18% for F = 0.99. Compared to the uncertainty of BC RI discussed in previous subsection, the uncertainty of RI of organics results in more uncertainties in the E_{ab}, which depicts much wider variation range.

3.4. Effect of Particle Size Distribution on E_{ab}

Figure 5 shows the variations of E_{ab} for partially coated BC aggregates (BC fractal dimension of ~2.8) with different particle size distributions at different shell/core ratios. The values of E_{ab} in accumulation mode (Figures 5a–5c) and in coarse mode (Figures 5d–5f) are depicted in Figure 5, respectively, and the panels from left to right correspond to three coated volume fractions of BC with F = 0.01, 0.5, and 0.99. The lognormal size distributions are assumed for the partially coated BC particles with r_g (x axis) ranging from 0.025 to 0.15 μm and 0.5 to 1.0 μm in accumulation and coarse mode, respectively, and σ_g fixed as the aforementioned values. Figure 5 clearly depicts that the E_{ab} of BC aggregates due to partially coated by organics is quite sensitive to particle size distribution, coated volume fraction of BC, and shell/core ratio. For accumulation coated BC with F = 0.01, the E_{ab} is in a range between 0.92 and 1.15 and shows weak variation on particle size distribution. It is interesting to see that the partially coated BC in accumulation mode with small coated volume fraction of BC exhibits E_{ab} slightly less than 1.0 for large particles (i.e., large r_g) with large D_p/D_c. Nevertheless, the variation of E_{ab} becomes stronger as the accumulation BC aerosols exhibit more coated volume fractions of BC, and their values vary in the ranges of 1.2–1.4 and 1.4–1.9 for F = 0.5 and F = 0.99, respectively. Comparing the results of all three coated volume fractions of BC, the E_{ab} of partially coated BC aggregates in accumulation mode becomes more sensitive to particle size distribution and shell/core ratio, i.e., showing larger variation, as coated volume fraction of BC becomes larger, and its value is in the range from ~1.0 to less than 2.0.

In Figures 5d–5f, the E_{ab} of partially coated BC in coarse mode shows similar patterns to those in accumulation mode, while the variations on particle size distribution and shell/core ratio become less complicated.

Compared to the accumulation mode, the E_{ab} of partially coated BC in coarse mode becomes less sensitive to particle size distribution and shell/core ratio and has much narrower ranges for all three coated volume fractions of BC. The E_{ab} of coarse partially coated BC aggregates is around 1.0 for $F = 0.01$, whereas its value is in a range between 1.1 and 1.3 for $F = 0.5$. When F is increased to 0.99, the E_{ab} of partially coated BC aggregates in coarse mode ranges from 1.4 to 1.7. Overall, in addition to shell/core ratio, Figure 5 indicates that the absorption enhancement of BC partially coated by organics is sensitive to both coated volume fraction of BC and size distribution, and the sensitivity of the absorption enhancement to particle size distribution becomes stronger as coated volume fraction of BC becomes larger and particles are in accumulation mode rather than coarse mode.

3.5. Atmospheric Implications

Our theoretical analysis has depicted the effects of aerosol microphysics (i.e., coated volume fraction of BC, particle shell/core ratio, BC refractive index, refractive index of organics, and size distribution) on the absorption enhancement of partially coated BC aggregates. It is documented that BC coating materials typically contain various inorganic species, such as sulfate and nitrate, in addition to organics (Guo et al., 2014). Since these nonabsorptive inorganic coating species generally have refractive indices similar to those of organics applied in our study, the results shown may have universal significance. Our results indicate that the absorption enhancements of partially coated BC particles are highly sensitive to their coated volume fraction of BC, and the coated volume fraction of BC seems to be responsible for the absorption enhancement. Meanwhile, the shell/core ratio, BC geometry, and size distribution have little impact on the E_{ab} of coated BC with small F, whereas they become significant for large F. The observations have shown large variability in BC coating morphology due to BC aging under different atmospheric conditions (China et al., 2013, 2015; Peng et al., 2016). Nevertheless, the detailed coating morphologies (such as shell/core ratio) responsible for E_{ab} may be considered only for coated BC with large coated volume fraction of BC (specifically, $F >$~0.5). Observationally, large diversities of the absorption enhancements, spanning from ~1.06 in California, USA (Cappa et al., 2012), to ~2.25 in the NCP (Cui et al., 2016), have been revealed. With highlighting the importance of accounting for the coated volume fraction of BC, our studies provide a plausible reconciliation of the conflicting results of largely variable absorption enhancements measured over different regions. Cappa et al. (2012) report that ambient E_{ab} observations stand in contrast to model formulations assuming a core-shell configuration and suggest that many climate models may overestimate warming by BC. Therefore, the partially coated BC model employed in our study may be considered in further studies, since the simplified core-shell model is only suitable for fully coated BC aerosols. Currently, the E_{ab} in aerosol-climate models has been commonly configured in the range of 1–2 (Chung & Seinfeld, 2005; He et al., 2014; Schulz et al., 2006), and this appears reasonable based on our study. However, a valuable addition to this is that the fully coated BC particles with high coating fractions may have the E_{ab} larger than 2, just as those observed in the NCP, where urban-scale photochemical production of sulfate, nitrate, and organics can happen (Chen et al., 2017). As such, this study suggests that a reliable estimate of the absorption enhancement of aged BC and then their radiative effects in aerosol-climate models would require the representation of realistic coating microphysics, especially the coated volume fraction of BC.

4. Conclusions

The study explores the impacts of coated volume fraction of BC, shell/core ratio, BC geometry, and size distribution on the absorption enhancements of BC aerosols partially coated by organics, as well as those externally attached and fully coated BC. The fractal aggregate is employed to model the realistic BC geometry, and its absorption enhancement after coating is calculated utilizing the numerically exact MSTM method. Our results indicate that the coated volume fraction of BC plays a significant role in determining the absorption enhancement of coated BC aggregates. The particle geometry, shell/core ratio, and size distribution have little impact on the E_{ab} of coated BC with small F, while they become significant for large F. The partially coated BC aerosols typically have an E_{ab} in the range of ~1.0–2.0, and it increases along with the increase of F for a fixed D_p/D_c, BC geometry, and size distribution. Surprisingly, the large partially coated BC particles with large D_p/D_c and small F in accumulation mode exhibit E_{ab} slightly less than 1.0, i.e., the absorption showing even slight decrease relative to uncoated BC particles. For partially coated BC aggregates in accumulation and coarse modes, the uncertainties of BC RI result in E_{ab} differences of less than 9% and 2%, respectively, and

more uncertainties are induced by different RI of organics with differences within 22% and 18%, respectively. Overall, this work presents that the internal particle morphology of coated BC particles can affect the extent to which absorption enhancements occur, which is consistent with suggestions from Adachi and Buseck (2013). Accounting for internal particle morphology, especially the coated volume fraction of BC, can potentially help to understand some of the differences in observations of coated BC absorption enhancements in various regions, although the extent to which variations in coating morphology provides a complete reconciliation remains to be determined. Another recent work by Fierce et al. (2016) also provides alternative plausible reconciliation, which show that accounting for the distribution of coating as a function of size, even within the core-shell framework, can also help to explain lower than anticipated absorption enhancements. Our study suggests that a reliable estimate of the absorption enhancement of aged BC particles and their radiative effects would require the representation of realistic coating microphysics, particularly the coated volume fraction of BC, in aerosol-climate models.

Acknowledgments

This work is financially supported by the National Natural Science Foundation of China (NSFC) (41505127 and 21406189), the Natural Science Foundation of Jiangsu Province (BK20150901), and the Natural Science Foundation of the Jiangsu Higher Education Institutions of China (15KJB170009). This work is also supported by the Startup Foundation for introducing Talent of NUIST (2015r002 and 2014r011), the China Postdoctoral Science Foundation Funded Project (2016 M591883), and the Jiangsu Planned Projects for Postdoctoral Research Funds (1601262C). We particularly acknowledge the source of the codes of MSTM 3.0 from Daniel W. Mackowski. All related data are available from the authors upon request (mmao@nuist.edu.cn) and are also deposited in https://mnmmz9.wixsite.com/xiaolin/data. We also gratefully appreciate the supports from Special Program for Applied Research on Super Computation of the NSFC-Guangdong Joint Fund (the second phase) under grant U1501501. This paper is ESMC Contribution No. 194.

References

Adachi, K., & Buseck, P. R. (2008). Internally mixed soot, sulfates, and organic matter in aerosol particles from Mexico City. *Atmospheric Chemistry and Physics*, *8*, 6469–6481. https://doi.org/10.5194/acp-8-6469-2008

Adachi, K., & Buseck, P. R. (2013). Changes of ns-soot mixing states and shapes in an urban area during CalNex. *Journal of Geophysical Research: Atmospheres*, *118*, 3723–3730. https://doi.org/10.1002/jgrd.50321

Alexander, D. T. L., Crozier, P. A., & Anderson, J. R. (2008). Brown carbon spheres in East Asian outflow and their optical properties. *Science*, *321*, 833–836. https://doi.org/10.1126/science.1155296

Bond, T. C., & Bergstrom, R. W. (2006). Light absorption by carbonaceous particles: An investigative review. *Aerosol Science and Technology*, *40*, 27–67. https://doi.org/10.1080/02786820500421521

Bond, T. C., Habib, G., & Bergstrom, R. W. (2006). Limitations in the enhancement of visible light absorption due to mixing state. *Journal of Geophysical Research*, *111*, D20211. https://doi.org/10.1029/2006JD007315

Bond, T. C., Doherty, S. J., Fahey, D. W., Forster, P. M., Berntsen, T., DeAngelo, B. J., … Zender, C. S. (2013). Bounding the role of black carbon in the climate system: A scientific assessment. *Journal of Geophysical Research: Atmospheres*, *118*, 5380–5552. https://doi.org/10.1002/jgrd.50171

Bueno, P. A., Havey, D. K., Mulholland, G. W., Hodges, J. T., Gillis, K. A., Dickerson, R. R., & Zachariah, M. R. (2011). Photoacoustic measurements of amplification of the absorption cross section for coated soot aerosols. *Aerosol Science and Technology*, *45*, 1217–1230. https://doi.org/10.1080/02786826.2011.587477

Cappa, C. D., Onasch, T. B., Massoli, P., Worsnop, D. R., Bates, T. S., Cross, E. S., … Zaveri, R. A. (2012). Radiative absorption enhancements due to the mixing state of atmospheric black carbon. *Science*, *337*, 1078–1081. https://doi.org/10.1126/science.1223447

Chakrabarty, R. K., Moosmuller, H., Chen, L. W. A., Lewis, K., Arnott, W. P., Mazzoleni, C., … Kreidenweis, S. M. (2010). Brown carbon in tar balls from smoldering biomass combustion. *Atmospheric Chemistry and Physics*, *10*, 6363–6370. https://doi.org/10.5194/acp-10-6363-2010

Chen, B., Bai, Z., Cui, X., Chen, J., Andersson, A., & Gustafsson, O. (2017). Light absorption enhancement of black carbon from urban haze in northern China winter. *Environmental Pollution*, *221*, 418–426. https://doi.org/10.1016/j.envpol.2016.12.004

Cheng, T., Gu, X., Wu, Y., & Chen, H. (2014). Effects of atmospheric water on the optical properties of soot aerosols with different mixing states. *Journal of Quantitative Spectroscopy & Radiative Transfer*, *147*, 196–206. https://doi.org/10.1016/j.jqsrt.2014.06.002

China, S., Mazzoleni, C., Gorkowski, K., Aiken, A. C., & Dubey, M. K. (2013). Morphology and mixing state of individual freshly emitted wildfire carbonaceous particles. *Nature Communications*, *4*(2122). https://doi.org/10.1038/ncomms3122

China, S., Scarnato, B., Owen, R. C., Zhang, B., Ampadu, M. T., Kumar, S., … Mazzoleni, C. (2015). Morphology and mixing state of aged soot particles at a remote marine free troposphere site: Implications for optical properties. *Geophysical Research Letters*, *42*, 1243–1250. https://doi.org/10.1002/2014GL062404

Chung, S. H., & Seinfeld, J. H. (2005). Climate response of direct radiative forcing of anthropogenic black carbon. *Journal of Geophysical Research*, *110*, D11102. https://doi.org/10.1029/2004JD005441

Coz, E., & Leck, C. (2011). Morphology and state of mixture of atmospheric soot aggregates during the winter season over Southern Asia—A quantitative approach. *Tellus B*, *63*, 107–116. https://doi.org/10.1111/j.1600-0889.2010.00513.x

Cui, X., Wang, X., Yang, L., Chen, B., Chen, J., Andersson, A., & Gustafsson, O. (2016). Radiative absorption enhancement from coatings on black carbon aerosols. *The Science of the Total Environment*, *551–552*, 51–56.

Dlugach, J. M., & Mishchenko, M. I. (2015). Scattering properties of heterogeneous mineral aerosols with absorbing inclussions. *Journal of Quantitative Spectroscopy & Radiative Transfer*, *162*, 89–94. https://doi.org/10.1016/j.jqsrt.2015.01.012

Dong, J., Zhao, J. M., & Liu, L. H. (2015). Morphological effects on the radiative properties of soot aerosols in different internally mixing states with sulfate. *Journal of Quantitative Spectroscopy & Radiative Transfer*, *165*, 43–55. https://doi.org/10.1016/j.jqsrt.2015.06.025

Draine, B. T., & Flatau, P. J. (1994). Discrete-dipole approximation for scattering calculations. *Journal of the Optical Society of America. A*, *11*(4), 1491–1499. https://doi.org/10.1364/JOSAA.11.001491

Fierce, L., Bond, T. C., Bauer, S. E., Mena, F., & Riemer, N. (2016). Black carbon absorption at the global scale is affected by particle-scale diversity in composition. *Nature Communications*, *7*, 12361. https://doi.org/10.1038/ncomms12361

Guo, S., Hu, M., Zamora, M. L., Peng, J. F., Shang, D. J., Zheng, J., … Zhang, R. Y. (2014). Elucidating severe urban haze formation in China. *Proceedings of the National Academy of Sciences of the United States of America*, *111*(49), 17,373–17,378. https://doi.org/10.1073/pnas.1419604111

He, C., Li, Q. B., Liou, K. N., Zhang, J., Qi, L., Mao, Y., … Ram, K. (2014). A global 3-D CTM evaluation of black carbon in the Tibetan plateau. *Atmospheric Chemistry and Physics*, *14*(13), 7091–7112. https://doi.org/10.5194/acp-14-7091-2014

He, C., Liou, K. N., Takano, Y., Zhang, R., Zamora, M. L., Yang, P., … Leung, L. R. (2015). Variation of the radiative properties during black carbon aging: Theoretical and experimental intercomparison. *Atmospheric Chemistry and Physics*, *15*(20), 11,967–11,980. https://doi.org/10.5194/acp-15-11967-2015

He, C., Takano, Y., Liou, K. N., Yang, P., Li, Q., & Mackowski, D. W. (2016). Intercomparison of the GOS approach, superposition T-matrix method, and laboratory measurements for black carbon optical properties during aging. *Journal of Quantitative Spectroscopy & Radiative Transfer*, *184*, 287–296. https://doi.org/10.1016/j.jqsrt.2016.08.004

Intergovernmental Panel on Climate Change (2013). *Climate Change: The Physical Science Basis*. UK: Cambridge University Press.

Khalizov, A. F., Xue, H., Wang, L., Zheng, J., & Zhang, R. (2009). Enhanced light absorption and scattering by carbon soot aerosol internally mixed with sulfuric acid. *The Journal of Physical Chemistry. A*, *113*(6), 1066–1074. https://doi.org/10.1021/jp807531n

Khalizov, A. F., Lin, Y., Qiu, C., Guo, S., Collins, D., & Zhang, R. Y. (2013). Role of OH-initiated oxidation of isoprene in aging of combustion soot. *Environmental Science & Technology*, *47*(5), 2254–2263. https://doi.org/10.1021/es3045339

Kim, H., & Paulson, S. E. (2013). Real refractive indices and volatility of secondary organic aerosol generated from photooxidation and ozonolysis of limonene, alpha-pinene and toluene. *Atmospheric Chemistry and Physics*, *13*(15), 7711–7723. https://doi.org/10.5194/acp-13-7711-2013

Knox, A., Evans, G. J., Brook, J. R., Yao, X., Jeong, C. H., Godri, K. J., … Slowik, J. G. (2009). Mass absorption cross-section of ambient black carbon aerosol in relation to chemical age. *Aerosol Science and Technology*, *43*, 522–532. https://doi.org/10.1080/02786820902777207

Li, W., Sun, J., Xu, L., Shi, Z., Riemer, N., Sun, Y., … Wang, W. (2016). A conceptual framework for mixing structures in individual aerosol particles. *Journal of Geophysical Research: Atmospheres*, *121*, 13,784–13,798. https://doi.org/10.1002/2016JD025252

Liou, K. N., & Yang, P. (2016). *Light Scattering by Ice Crystals: Fundamentals and Applications* (pp. 168–173). Cambridge, UK: Cambridge University Press. https://doi.org/10.1017/CBO9781139030052

Liou, K. N., Takano, Y., He, C., Yang, P., Leung, L. R., Gu, Y., & Lee, W. L. (2014). Stochastic parameterization for light absorption by internally mixed BC/dust in snow grains for application to climate models. *Journal of Geophysical Research: Atmospheres*, *119*, 7616–7632. https://doi.org/10.1002/2014JD021665

Liu, L., & Mishchenko, M. I. (2007). Scattering and radiative properties of complex soot and soot-containing aggregate particles. *Journal of Quantitative Spectroscopy & Radiative Transfer*, *106*, 262–273. https://doi.org/10.1016/j.jqsrt.2007.01.020

Liu, L., Mishchenko, M. I., & Arnott, W. P. (2008). A study of radiative properties of fractal soot aggregates using the superposition T-matrix method. *Journal of Quantitative Spectroscopy & Radiative Transfer*, *109*, 2656–2663. https://doi.org/10.1016/j.jqsrt.2008.05.001

Liu, D., Taylor, J. W., Young, D. E., Flynn, M. J., Coe, H., & Allan, J. D. (2015). The effect of complex black carbon microphysics on the determination of the optical properties of brown carbon. *Geophysical Research Letters*, *42*, 613–619. https://doi.org/10.1002/2014GL062443

Liu, S., Aiken, A. C., Gorkowski, K., Dubey, M. K., Cappa, C. D., Williams, L. R., … Prevot, A. S. H. (2015). Enhanced light absorption by mixed source black and brown carbon particles in UK winter. *Nature Communications*, *6*, 8435. https://doi.org/10.1038/ncomms9435

Liu, F., Yon, J., & Bescond, A. (2015). On the radiative properties of soot aggregates - Part2: Effects of coating. *Journal of Quantitative Spectroscopy & Radiative Transfer*, *172*, 134–145.

Mackowski, D. W. (2014). A general superposition solution for electromagnetic scattering by multiple spherical domains of optically active media. *Journal of Quantitative Spectroscopy & Radiative Transfer*, *133*, 264–270. https://doi.org/10.1016/j.jqsrt.2013.08.012

Mackowski, D. W., & Mishchenko, M. I. (1996). Calculation of the T matrix and the scattering matrix for ensembles of spheres. *Journal of the Optical Society of America. A*, *13*(11), 2266–2278. https://doi.org/10.1364/JOSAA.13.002266

Mao, M., Zhang, X., Fang, X., Wu, G., Dai, S., Song, Q., & Zhang, X. (2014). Highly efficient light-harvesting boradiazaindacene sensitizers for dye-sensitized solar cells featuring phenothiazine donor antenna. *Journal of Power Sources*, *268*, 965–976. https://doi.org/10.1016/j.jpowsour.2014.05.079

Mishchenko, M. I., Dlugach, J. M., Yurkin, M. A., Bi, L., Cairns, B., Liu, L., … Zakharova, N. (2016). First-principles modeling of electromagnetic scattering by discrete and discretely heterogeneous random media. *Physics Reports*, *632*, 1–75. https://doi.org/10.1016/j.physrep.2016.04.002

Myhre, G. (2009). Consistency between satellite-derived and modeled estimates of the direct aerosol effect. *Science*, *325*, 187–190. https://doi.org/10.1126/science.1174461

Naoe, H., Hasegawa, S., Heintzenberg, J., Okada, K., Uchiyama, A., Zaizen, Y., … Yamazaki, A. (2009). State of mixture of atmospheric submicrometer black carbon particles and its effect on particulate light absorption. *Atmospheric Environment*, *43*, 1296–1301. https://doi.org/10.1016/j.atmosenv.2008.11.031

Peng, J., Hua, M., Guo, S., Du, Z., Zheng, J., Shang, D., … Zhang, R. (2016). Markedly enhanced absorption and direct radiative forcing of black carbon under polluted urban environments. *Proceedings of the National Academy of Sciences of the United States of America*, *113*(16), 4266–4271. https://doi.org/10.1073/pnas.1602310113

Qiu, C., Khalizov, A. F., & Zhang, R. (2012). Soot aging from OH-initiated oxidation of toluene. *Environmental Science & Technology*, *46*, 9464–9472. https://doi.org/10.1021/es301883y

Ramanathan, V., & Carmichael, G. (2008). Global and regional climate changes due to black carbon. *Nature Geoscience*, *1*, 221–227. https://doi.org/10.1038/ngeo156

Scarnato, B. V., China, S., Nielsen, K., & Mazzoleni, C. (2015). Perturbations of the optical properties of mineral dust particles by mixing with black carbon: A numerical simulation study. *Atmospheric Chemistry and Physics*, *15*(12), 6913–6928. https://doi.org/10.5194/acp-15-6913-2015

Schulz, M., Textor, C., Kinne, S., Balkanski, Y., Bauer, S., Berntsen, T., … Takemura, T. (2006). Radiative forcing by aerosols as derived from the AeroCom present-day and pre-industrial simulations. *Atmospheric Chemistry and Physics*, *6*, 5225–5246. https://doi.org/10.5194/acp-6-5225-2006

Schwarz, J. P., Spackman, J. R., Fahey, D. W., Gao, R. S., Lohmann, U., Stier, P., … Reeves, J. M. (2008). Coatings and their enhancement of black carbon light absorption in the tropical atmosphere. *Journal of Geophysical Research*, *113*, D03203. https://doi.org/10.1029/2007JD009042

Shiraiwa, M., Kondo, Y., Iwamoto, T., & Kita, K. (2010). Amplification of light absorption of black carbon by organic coating. *Aerosol Science and Technology*, *44*, 46–54. https://doi.org/10.1080/02786820903357686

Skorupski, K., Mroczka, J., Wriedt, T., & Riefler, N. (2014). A fast and accurate implementation of tunable algorithms used for generation of fractal-like aggregate models. *Physica A*, *404*, 106–117. https://doi.org/10.1016/j.physa.2014.02.072

Sorensen, C. M. (2001). Light scattering by fractal aggregates: A review. *Aerosol Science and Technology*, *35*(2), 648–687. https://doi.org/10.1080/02786820117868

Tritscher, T., Juranyi, Z., Martin, M., Chirico, R., Gysel, M., Heringa, M. F., … Baltensperger, U. (2011). Changes of hygroscopicity and morphology during ageing of diesel soot. *Environmental Research Letters*, *6*, 034026. https://doi.org/10.1088/1748-9326/6/3/034026

Wang, Q., Huang, R., Cao, J., Han, Y., Wang, G., Li, G., … Zhou, Y. (2014). Mixing state of black carbon aerosol in a heavily polluted urban area of China: Implications for light absorption enhancement. *Aerosol Science and Technology*, *48*(7), 689–697. https://doi.org/10.1080/02786826.2014.917758

Wang, G., Zhang, R., Gomez, M. E., Yang, L., Zamora, M. L., Hu, M., … Molina, M. J. (2016). Persistent sulfate formation from London fog to Chinese haze. *Proceedings of the National Academy of Sciences of the United States of America*, *113*(48), 13,630–13,635. https://doi.org/10.1073/pnas.1616540113

Wu, Y., Cheng, T. H., Zheng, L. J., & Chen, H. (2016). Optical properties of the semi-external mixture composed of sulfate particle and different quantities of soot aggregates. *Journal of Quantitative Spectroscopy & Radiative Transfer*, *179*, 139–148. https://doi.org/10.1016/j.jqsrt.2016.03.012

Xue, H., Khalizov, A. F., Wang, L., Zheng, J., & Zhang, R. (2009). Effects of dicarboxylic acid coating on the optical properties of soot. *Physical Chemistry Chemical Physics*, *11*, 7869–7875. https://doi.org/10.1039/b904129j

Yang, P., & Liou, K. N. (1996). Finite-difference time domain method for light scattering by small ice crystals in three-dimensional space. *Journal of the Optical Society of America. A*, *13*(10), 2072–2085. https://doi.org/10.1364/JOSAA.13.002072

Yurkin, M. A., & Hoekstra, A. G. (2007). The discrete dipole approximation: An overview and recent developments. *Journal of Quantitative Spectroscopy & Radiative Transfer*, *106*, 558–589. https://doi.org/10.1016/j.jqsrt.2007.01.034

Zhang, X., & Mao, M. (2015). Brown haze types due to aerosol pollution at Hefei in the summer and fall. *Chemosphere*, *119*, 1153–1162. https://doi.org/10.1016/j.chemosphere.2014.08.038

Zhang, R., Khalizov, A. F., Pagels, J., Zhang, D., Xue, H., & McMurry, P. H. (2008). Variability in morphology, hygroscopicity, and optical properties of soot aerosols during atmospheric processing. *Proceedings of the National Academy of Sciences of the United States of America*, *105*, 10,291–10,296. https://doi.org/10.1073/pnas.0804860105

Zhang, K., O'Donnell, D., Kazil, J., Stier, P., Kinne, S., Lohmann, U., … Feichter, J. (2012). The global aerosol-climate model ECHAM-HAM, version 2: Sensitivity to improvements in process representations. *Atmospheric Chemistry and Physics*, *12*, 8911–8949. https://doi.org/10.5194/acp-12-8911-2012

Zhang, X., Huang, Y., & Rao, R. (2012). Aerosol characteristics including fumigation effect under weak precipitation over the southeastern coast of China. *Journal of Atmospheric and Solar: Terrestrial Physics*, *84–85*, 25–36.

Zhang, X., Huang, Y., Rao, R., & Wang, Z. (2013). Retrieval of effective complex refractive index from intensive measurements of characteristics of ambient aerosols in the boundary layer. *Optics Express*, *21*(15), 17,849–17,862. https://doi.org/10.1364/OE.21.017849

Zhang, X., Huang, Y., Zhu, W., & Rao, R. (2013). Aerosol characteristics during summer haze episodes from different source regions over the coast city of North China Plain. *Journal of Quantitative Spectroscopy & Radiative Transfer*, *122*, 180–193. https://doi.org/10.1016/j.jqsrt.2012.08.009

Zhang, X., Mao, M., Berg, M. J., & Sun, W. (2014). Insight into wintertime aerosol characteristics over Beijing. *Journal of Atmospheric and Solar: Terrestrial Physics*, *121*, 63–71. https://doi.org/10.1016/j.jastp.2014.09.017

Zhang, X., Rao, R., Huang, Y., Mao, M., Berg, M. J., & Sun, W. (2015). Black carbon aerosols in urban central China. *Journal of Quantitative Spectroscopy & Radiative Transfer*, *150*, 3–11. https://doi.org/10.1016/j.jqsrt.2014.03.006

Zhang, Y., Zhang, Q., Cheng, Y., Su, H., Kecorius, S., Wang, Z., … He, K. (2016). Measuring the morphology and density of internally mixed black carbon with SP2 and VTDMA: New insight into the absorption enhancement of black carbon in the atmosphere. *Atmospheric Measurement Techniques*, *9*(4), 1833–1843. https://doi.org/10.5194/amt-9-1833-2016

Zhang, X., Mao, M., Yin, Y., & Wang, B. (2017). Absorption enhancement of aged black carbon aerosols affected by their microphysics: A numerical investigation. *Journal of Quantitative Spectroscopy & Radiative Transfer*, *202*, 90–97. https://doi.org/10.1016/j.jqsrt.2017.07.025